Supp. Fig. 1

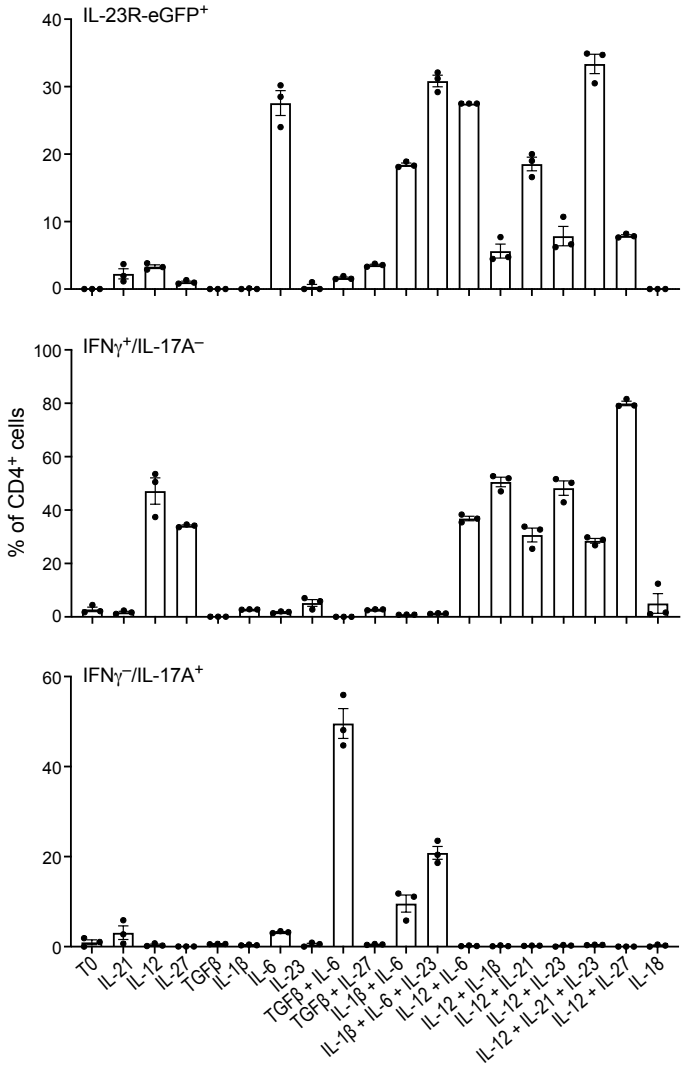
IL-23R-eGFP+
IFNγ+/IL-17A−
IFNγ−/IL-17A+
% of CD4+ cells
T0
IL-21
IL-12
IL-27
TGFβ
IL-1β
IL-6
IL-23
TGFβ + IL-6
TGFβ + IL-27
IL-1β + IL-6
IL-1β + IL-6 + IL-23
IL-12 + IL-6
IL-12 + IL-18
IL-12 + IL-21
IL-12 + IL-23
IL-12 + IL-21 + IL-23
IL-12 + IL-27
IL-18

Figure S1, refers to figure 1. Cytokine screen identifies IL-21 as a cytokine that together with IL-12 induces strong expression of IL-23R in Th1-like cells *in vitro*. Naïve T cells from *Il23r*$^{wt/eGFP}$ reporter mice were differentiated with 19 different cytokine conditions. Flow cytometry analysis of IL-23R expression by identifying eGFP^{+} cells and IFN-γ and IL-17A expression by intracellular cytokine staining. Both IL-12 + IL-21 and IL-12 + IL-21 + IL-23 induced the expression of IL-23R and IFN-γ with no IL-17A expression. Data are representative of several independent experiments. Technical replicates are shown (n=3).

Supp. Fig. 2

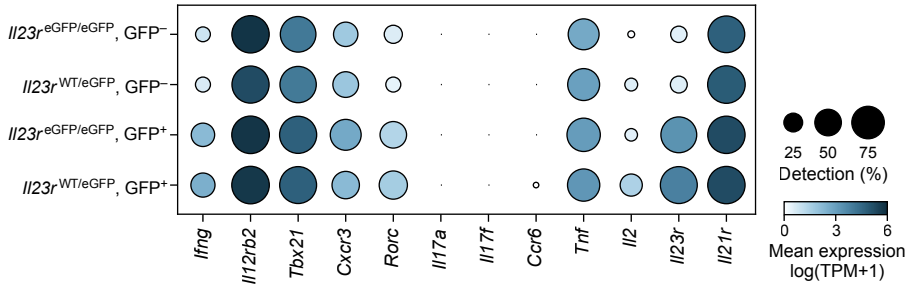
Il23r eGFP/eGFP, GFP−
Il23r WT/eGFP, GFP−
Il23r eGFP/eGFP, GFP+
Il23r WT/eGFP, GFP+
Ifng
Il12rb2
Tbx21
Cxcr3
Rorc
Il17a
Il17f
Ccr6
Tnf
Il2
Il23r
Il21r
25 50 75
Detection (%)
0 3 6
Mean expression
log(TPM+1)

Figure S2, refers to figure 1. Expression of key Th1 and Th17 cell genes across the 4 populations profiled by smart-seq2. *Tbx21*, *Il12rb2* and *Il21r* expression appeared largely unaltered by deficiency for *Il23r* which was consistent with unaltered expression between $eGFP^+$ and $eGFP^-$ populations. Of note, *Il23r* expression in IL-23R-deficient cells (*Il23r*$^{eGFP/eGFP}$) is due to the cells producing mRNA truncated of the essential C-terminal region of IL-23R which was replaced by an *IRES-eGFP* sequence. This results in a loss-of-function allele but is detected by smart-seq2.

Supp. Fig. 3

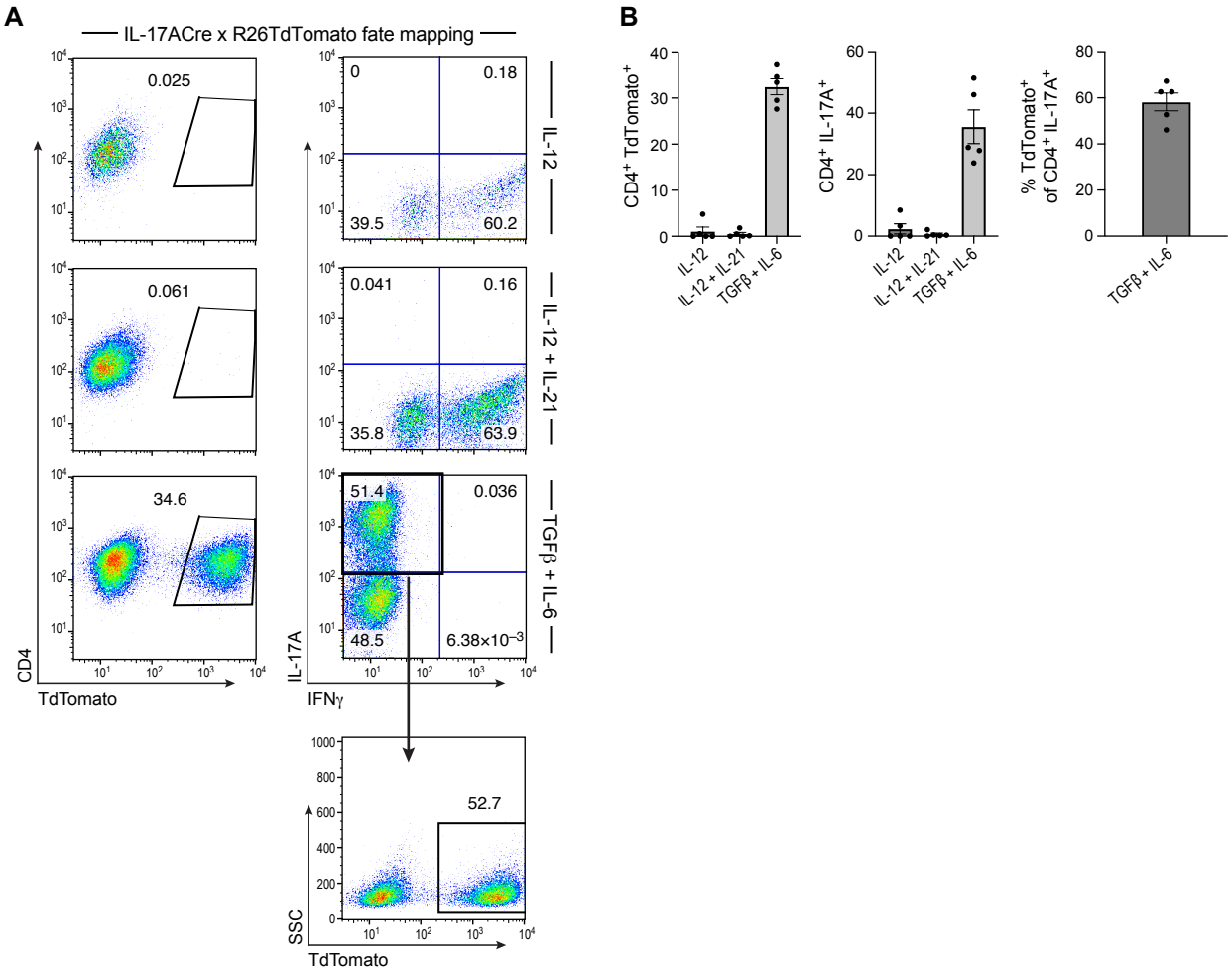
A
IL-17ACre x R26TdTomato fate mapping
0.025
0.061
34.6
CD4
TdTomato
0
0.18
39.5
60.2
0.041
0.16
35.8
63.9
51.4
0.036
48.5
6.38×10−3
IL-17A
IFNγ
IL-12
IL-12 + IL-21
TGFβ + IL-6
52.7
SSC
TdTomato
B
CD4+ TdTomato+
CD4+ IL-17A+
% TdTomato+ of CD4+ IL-17A+
IL-12
IL-12 + IL-21
TGFβ + IL-6

Figure S3, refers to figures 1 and 2. IL-17ACre (Th17 cell) fate mapping in naïve T cells differentiated under various cytokine conditions *in vitro*. (A) Naïve T cells from Th17 cell fate mapping mice (IL-17A$^{Cre/+}$; ROSA26^{TdTomato}) were differentiated under the following conditions: (1) IL-12 (Th1 cells); (2) IL-12 + IL-21; (3) TGF-β + IL-6 (non-pathogenic Th17 cells).

TdTomato expression was further investigated in the IL-17A^{+}IFN-γ^{-} population of the TGF-β + IL-6 condition. (B) Data pooled from two independent experiments are shown. Mean ± s.e.m.

Supp. Fig. 4

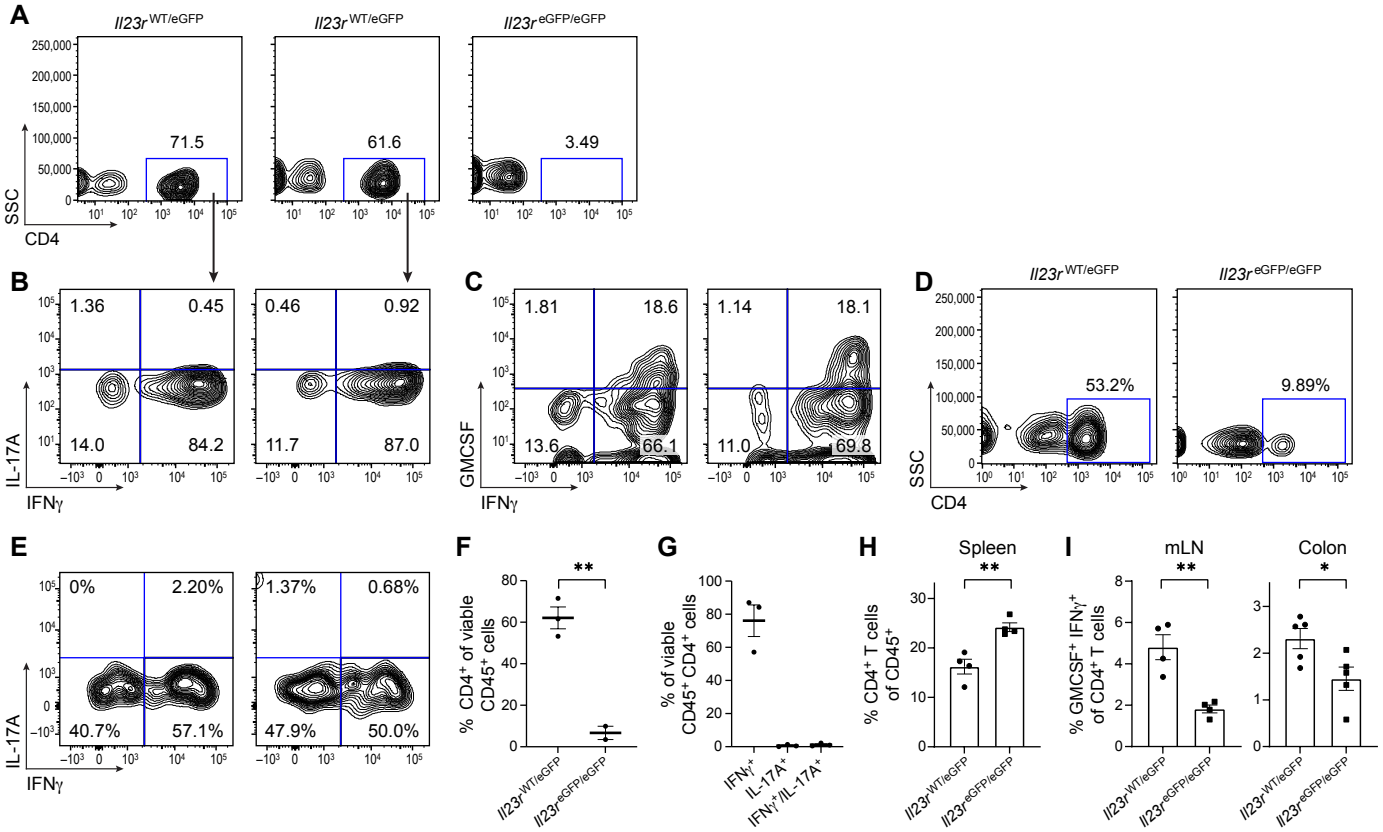
A
Il23r WT/eGFP
Il23r WT/eGFP
Il23r eGFP/eGFP
71.5
61.6
3.49
SSC
CD4
B
1.36
0.45
14.0
84.2
0.46
0.92
11.7
87.0
IL-17A
IFNγ
C
1.81
18.6
13.6
66.1
1.14
18.1
11.0
69.8
GMCSF
IFNγ
D
Il23r WT/eGFP
Il23r eGFP/eGFP
53.2%
9.89%
SSC
CD4
E
0%
2.20%
40.7%
57.1%
1.37%
0.68%
47.9%
50.0%
IL-17A
IFNγ
F
% CD4+ of viable CD45+ cells
**
Il23rWT/eGFP
Il23reGFP/eGFP
G
% of viable CD45+CD4+ cells
IFNγ+
IL-17A+
IFNγ+/IL-17A+
H
Spleen
**
% CD4+ T cells of CD45+
Il23rWT/eGFP
Il23reGFP/eGFP
I
mLN
**
Colon
*
% GMCSF+ IFNγ+ of CD4+ T cells
Il23rWT/eGFP
Il23reGFP/eGFP

Figure S4, refers to figure 4. Tissue infiltrating CD45$^+$CD4$^+$ T cells show high expression of IFN-γ. Flow cytometric analysis of tissue infiltrating T cells isolated from the intestine of *Rag1*$^{-/-}$ recipients of wildtype or IL-23R KO cells and cultured overnight with the cytokines IL-7 + IL-23 (A-G). (A) Colonic LPL cells. Two recipients of wildtype cells (*Il23r*$^{eGFP/wt}$) and one recipient of KO cells (*Il23r*$^{eGFP/eGFP}$) are shown. Gated on viable CD45$^+$ cells. (B) and (C) ICC for IFN-γ, IL-17A and GM-CSF of the two recipients of wildtype cells. (D) Colonic IEL cells. One recipient of wildtype cells and one recipient of KO cells are shown. Gated on viable CD45$^+$ cells. (E) ICC for IFN-γ and IL-17A of the IEL samples. (F) and (G) Pooled values of LPL and IEL samples. LPL and IEL samples were isolated in independent experiments and combined for analysis. Data in panels (F) and (G) are mean ± s.e.m. Unpaired t-test, $p < 0.01$** in panel (F). (H) and (I) CD4$^+$ T cells were isolated from recipients of either IL-23R-competent or IL-23R-deficient cells and investigated without overnight culture. (H) Quantification of CD45$^+$CD4$^+$ T cells in the spleen of *Rag1*$^{-/-}$ recipients. (I) ICC and quantification of GM-CSF$^+$IFN-γ$^+$ CD4$^+$ T cells in mesenteric lymph nodes and colon, respectively. Mean ± s.e.m. are shown. T-test. $p < 0.05$*, $p < 0.01$**.

Supp. Fig. 5

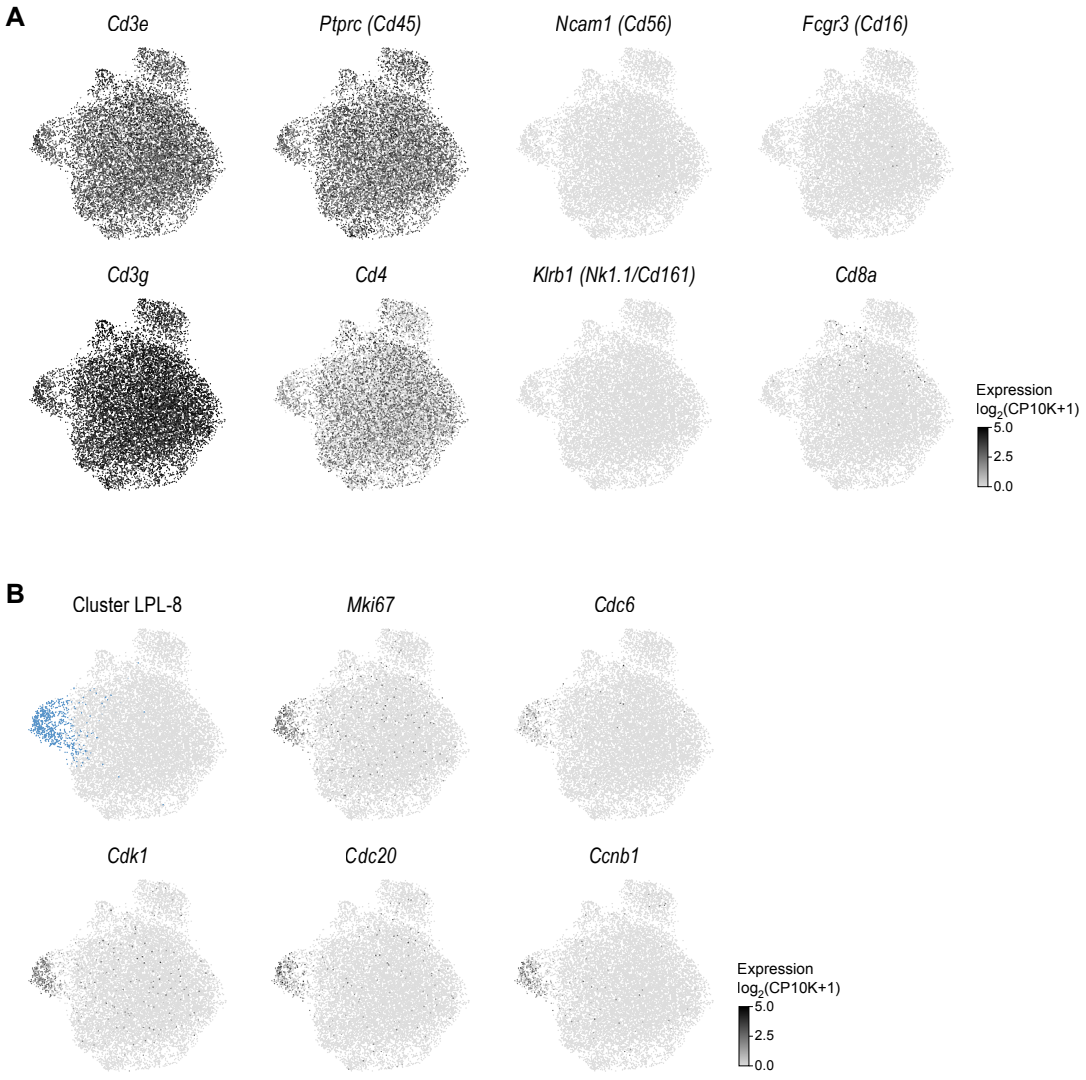
A
Cd3e
Ptprc (Cd45)
Ncam1 (Cd56)
Fcgr3 (Cd16)
Cd3g
Cd4
Klrb1 (Nk1.1/Cd161)
Cd8a
Expression
log2(CP10K+1)
5.0
2.5
0.0
B
Cluster LPL-8
Mki67
Cdc6
Cdk1
Cdc20
Ccnb1
Expression
log2(CP10K+1)
5.0
2.5
0.0

Figure S5, refers to figure 5. Expression of T cell, NK cell and proliferation markers in scRNAseq of cells isolated from the intestinal mucosa (LPL). (A) UMAPs depicting the expression of CD45, CD3, CD4 and lack of expression of NK cell markers (NK1.1, CD56 and CD16) and CD8a.

(B) Cluster 8 represents proliferating cells. UMAPs showing the expression of cell cycle genes in cluster 8 (*Cdc20*, *Ccnb1* (cyclin B), *Cdc6*, *Cdk1*, *Mki67*).

Supp. Fig. 6

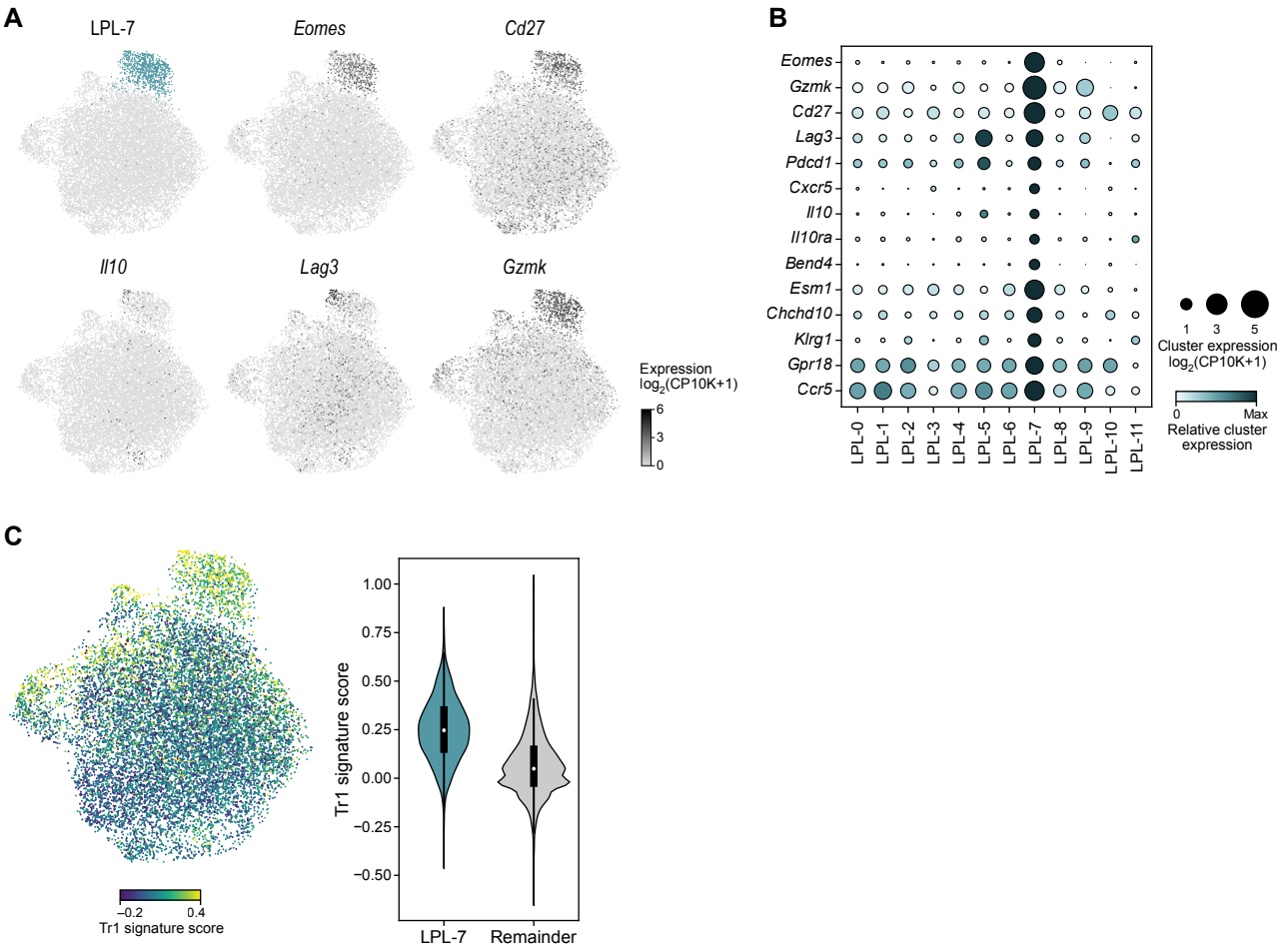
A
LPL-7
Eomes
Cd27
Il10
Lag3
Gzmk
Expression
log2(CP10K+1)
6
3
0
B
Eomes
Gzmk
Cd27
Lag3
Pdcd1
Cxcr5
Il10
Il10ra
Bend4
Esm1
Chchd10
Klrg1
Gpr18
Ccr5
LPL-0
LPL-1
LPL-2
LPL-3
LPL-4
LPL-5
LPL-6
LPL-7
LPL-8
LPL-9
LPL-10
LPL-11
1
3
5
Cluster expression
log2(CP10K+1)
0
Max
Relative cluster
expression
C
−0.2
0.4
Tr1 signature score
1.00
0.75
0.50
0.25
0.00
−0.25
−0.50
Tr1 signature score
LPL-7
Remainder

Figure S6, refers to figure 5. IL-23R negatively impacts the development of regulatory Tr1 cells in the intestinal lamina propria as identified by scRNAseq. (A) UMAPs and correlated expression profiles of signature genes of regulatory Tr1 cells marking cluster 7. (B) Dot plot showing the expression of selected signature genes in comparison to all other clusters. (C) Transcriptional signature of human Tr1 regulatory cells (Gruarin *et al.*, 2019) highlights cluster 7.

Supp. Fig. 7

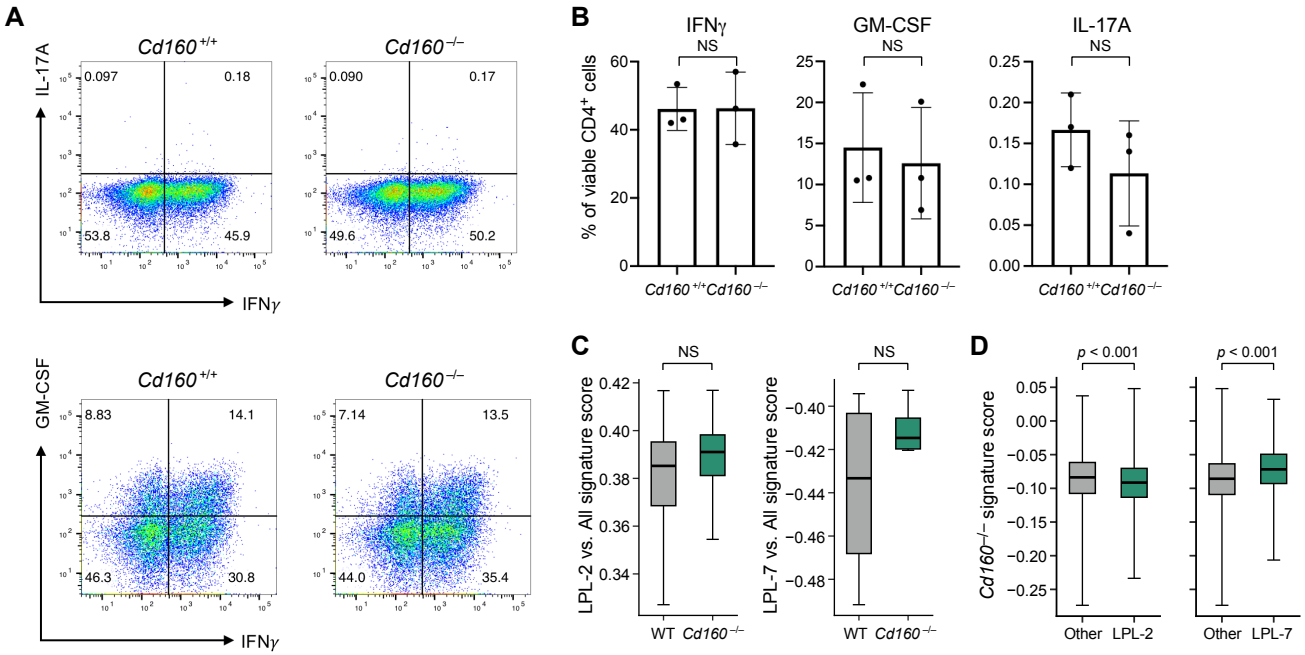
A
Cd160+/+
Cd160−/−
IL-17A
IFNγ
0.097
0.18
53.8
45.9
0.090
0.17
49.6
50.2
GM-CSF
8.83
14.1
46.3
30.8
7.14
13.5
44.0
35.4
B
IFNγ
GM-CSF
IL-17A
NS
% of viable CD4+ cells
Cd160+/+Cd160−/−
C
LPL-2 vs. All signature score
LPL-7 vs. All signature score
WT Cd160−/−
D
p < 0.001
Cd160−/− signature score
Other LPL-2
Other LPL-7

Figure S7, refers to figures 6 and 7. *In vitro* differentiated Th1-like cells from either *Cd160*$^{+/+}$ or *Cd160*$^{-/-}$ cells do not show a difference in IFN-γ expression prior to adoptive transfer. Naïve T cells differentiated with IL-12 + IL-21 + IL-23. (A) One representative experiment of three independent experiments is shown. (B) Pooled data from 3 independent experiments are shown. Mean ± SD are shown. T-test. NS: Not significant. (C) Alternate comparisons to that of Figure 7F. Signature scores computed using the genes distinguishing LPL clusters 2 and 7 from other clusters (Figure 5) on wildtype and *Cd160*$^{-/-}$ population RNAseq samples. (D) Alternate comparisons to that of Figure 7G. A signature created from the *Cd160*$^{-/-}$ vs. wildtype comparison was used to score lamina propria lymphocytes from the single-cell results (Figure 5). Statistical analysis for panels (C-D), see methods.